Available online at www.sciencedirect.com
SCIENCE DIRECT®
Atmospheric Environment 40 (2006) 1464–1479
ATMOSPHERIC ENVIRONMENT
www.elsevier.com/locate/atmosenv

Development of species-based, regional emission capacities for simulation of biogenic volatile organic compound emissions in land-surface models: An example from Texas, USA

Lindsey E. Gulden, Zong-Liang Yang*

Department of Geological Sciences, The John A. and Katherine G. Jackson School of Geosciences, University of Texas at Austin, 1 University Station #C1100, Austin, TX 78712-0254, USA

Received 13 July 2005; received in revised form 20 October 2005; accepted 22 October 2005

Abstract

This paper introduces a method to incorporate species-based variation of the emission of biogenic volatile organic compounds (BVOCs) into regional climate and weather models. We convert a species-based land-cover database for Texas into a database compatible with the community land model (CLM) and a database compatible with the Noah land-surface model (LSM). We link the LSM-compatible land-cover databases to the original species-based data set as a means to derive region-specific BVOC emission capacities for each plant functional type (in the CLM database) and for each land-cover type (in the Noah database).

The spatial distribution of inherent BVOC flux (defined as the product of the BVOC emission capacity and the leaf biomass density) derived using the Texas-specific BVOC emission capacities is well correlated with the spatial distribution of inherent BVOC flux calculated using the original species data ($r = 0.89$). The mean absolute error for the emission-capacity-derived inherent flux distribution is an order of magnitude lower than the statewide range of inherent fluxes.

The ground-referenced land-cover databases derived here are likely more accurate than their satellite-derived counterparts; they can be used for a variety of regional model simulations in Texas. The inherent BVOC flux distributions derived using region-specific BVOC emission capacities are more consistent with observations than the BVOC flux distribution derived using the CLM3 standard BVOC emission capacities, which are top-down estimates based on the literature. When used in conjunction with detailed land-cover data sets, region-specific BVOC emission capacities produce reasonably accurate inherent BVOC fluxes.

Keywords: BVOC; Biogenic emissions; Regional climate models; Regional weather models; Emission capacity

1. Introduction

Comprehensive, stand-alone models of the climate system require the accurate simulation of processes that involve biogenic emissions. Biogenic volatile organic compounds (BVOCs) are messengers between the land surface and atmosphere. Atmospheric conditions influence the rate at which BVOCs are emitted to the atmosphere, and BVOCs, in turn, influence atmospheric chemistry, cloud formation, Earth's radiative balance, and the global carbon cycle.

*Corresponding author. Tel.: +1 512 471 3824; fax: +1 512 471 9425.
E-mail address: liang@mail.utexas.edu (Z.-L. Yang).

1352-2310/$ - see front matter © 2005 Elsevier Ltd. All rights reserved.
doi:10.1016/j.atmosenv.2005.10.046

The long-term pattern of atmospheric variation determines the composition of plant species that covers the land surface; vegetation species exerts primary control on the magnitude of BVOC flux. On a shorter time scale, variation in atmospheric conditions determines the amount of photosynthetic active radiation (PAR) reaching the leaf surface, leaf-surface temperature, and soil moisture, all of which influence variation in BVOC emissions (e.g., Guenther et al., 1991; Plaza et al., 2005). Once emitted to the atmosphere, BVOCs react in the presence of nitrogen oxides to increase the concentration of tropospheric ozone (e.g., Wiedinmyer et al., 2001a, b), which is a respiratory irritant and major component of smog. The oxidation products of both isoprene and non-isoprene BVOCs condense to form secondary organic aerosols (Claeys et al., 2004; Kavouras et al., 1998), which directly alter Earth's radiative balance and can serve as cloud-condensation nuclei (Andreaevc and Crutzen, 1997). Most BVOCs are precursors to atmospheric carbon dioxide and are thus a mechanism for carbon exchange between the land surface and the atmosphere (e.g., Guenther, 2002). The magnitude of the BVOC flux between the land surface and atmosphere is considerable: Guenther et al. (1995) estimate that the combined global BVOC emissions contribute 1150 Tg of carbon to the atmosphere each year.

Large-scale study of land-surface–atmosphere feedbacks that involve biogenic emissions requires that BVOC fluxes be accurately represented within land-surface models (LSMs), which serve as the lower boundary for weather and climate models. The ability of LSMs to correctly represent BVOC flux limits the value of future improvements to weather and climate models' parameterizations of BVOC-related atmospheric processes.

The dependence of BVOC emission on plant species poses a significant obstacle to the accurate representation of biogenic emissions within LSMs. Although changes in environmental conditions cause the greatest variation in the quantity of BVOCs emitted from a single plant, interspecies variation in BVOC emission capacity exerts primary control on the differences in the rates at which disparate landscapes emit BVOCs. Current-generation LSMs represent vegetation either as static land-cover classes (e.g., as in the Noah LSM; Chen and Dudhia, 2001) or as mosaics of plant functional types (PFTs), such as "temperate needleleaf evergreen tree" and "temperate broadleaf deciduous shrub" (e.g., as in the community land model (CLM) version 3; Oleson et al., 2004; Bonan et al., 2002). The vast number of species represented by a single LSM land-cover type makes accurate representation of BVOC fluxes using LSM land-cover types a challenge.

In their BVOC emissions module, which is standard within CLM3, Levis et al. (2003) (hereafter, "Levis et al.") represent broad-scale interspecies variability in BVOC emissions by assigning unique emission capacities to each PFT. They base their emissions module on the work of Guenther et al. (1995), who modeled BVOC flux as a function of foliar density, PAR, leaf-surface temperature, and an ecosystem-specific emission capacity. For a given PFT, Levis et al. represent the emission of BVOC type i (isoprene, monoterpene, other volatile organic compounds [OVOCs], other reactive volatile organic compounds [ORVOCs], or CO) as

$$F_i = \varepsilon_i D(L_{\text{sun}} + L_{\text{shade}})_i T_i, \quad (1)$$

where F_i is the flux to the atmosphere of BVOC type i (units: $\mu g\,C\,m^{-2}\,h^{-1}$), D the foliar density (units: g dry leaf matter (gdlm) m^{-2} of ground covered by the PFT), ε_i a PFT-specific emission capacity (units: $\mu g\,C\,gdlm^{-1}\,h^{-1}$), L_{sun} and L_{shade} are dimensionless factors that modulate BVOC emissions from sunlit and shaded leaves in response to changes in PAR, and T_i is a dimensionless factor that adjusts BVOC flux in response to changes in canopy temperature.

Global observational estimates of total BVOC emissions do not yet exist; however, the magnitude and spatial variability of the global BVOC flux simulated offline by Levis et al.'s module are consistent with other model estimates (e.g., Guenther et al., 1995). When Levis et al. simulated BVOC emissions at $3.75^\circ \times 3.75^\circ$ resolution for 10 model years using the fully coupled community climate system model with dynamic vegetation, interannual variability in total BVOC flux reached 29%. This is consistent with the work of Abbot et al. (2003), who used space-based atmospheric column measurements of formaldehyde as a proxy for isoprene emissions over North America. The scientists found that between 1995 and 2001, interannual variability in estimated isoprene emissions was ~30% (Abbot et al., 2003); the spatial distribution and magnitude of their estimated isoprene emissions generally matched the predictions of models with emissions parameterizations similar to that of Levis et al. Plot-scale observational studies also report appreciable interannual variation in BVOC emission (e.g., Hakola et al., 2003).

Levis et al. used globally constant PFT-specific emission capacities. The "top-down" assignment of PFT-specific emissions capacities is a defensible simplification for qualitative global simulations but is likely insufficient for regional simulations. Levis et al. suggest using region-specific emission capacities as a way to increase the accuracy with which CLM3 simulates BVOC fluxes on a regional scale. Here, we present a "bottom-up" method for determining Texas-specific BVOC emission capacities for PFTs using a species-based, ground-referenced land-cover database (Wiedinmyer et al., 2001b). We also apply this method to develop regional BVOC emission capacities for the static land-cover types used in the Noah LSM, which is used as the lower boundary for the fifth-generation Penn State/NCAR Mesoscale Model (MM5) (Grell et al., 1995) and for the weather research and forecasting (WRF) model (Skamarock et al., 2005). CLM is an LSM representative of those used in climate model simulations; the Noah LSM is widely used in both the weather- and climate-modeling communities. Methods described here can be applied to other LSMs as research needs dictate.

In this paper, we address only the BVOC emission capacity of the land surface. We do not report simulation results. Unique contributions of this study are (1) the development of two ground-referenced, species-based, 1-km land-cover databases for Texas that can be used as input to LSMs (CLM and Noah) and (2) the demonstration and evaluation of a method for deriving region-specific BVOC emission capacities for use in regional climate and weather models.

2. Data and methods

2.1. The Wiedinmyer database

The Wiedinmyer et al. (2001b) database describes the Texas landscape using 600+ species-based land-cover classes. Wiedinmyer and colleagues developed the database as input to an MS Access-based BVOC emissions module, GLOBEIS (http://www.globeis.com; Yarwood et al., 1999). Where BVOC emissions are typically high (in eastern and central Texas), the researchers conducted field surveys to determine species composition and density information. The researchers then mapped that information to the land-cover classes contained in 10 existing, often overlapping land-cover databases for various regions in Texas. A detailed description of the methods used to develop the data set can be found in Wiedinmyer et al. (2000, 2001b).

The resolution of the Wiedinmyer database is ~1 km; some urban areas have a finer resolution. We employed ESRI's ArcGIS software to convert the original Wiedinmyer database to a uniform $1 \times 1\text{-km}^2$ gridded data set.

Each Wiedinmyer land-cover class contains species composition information. One class contains between 1 and 115 of 289 possible component species. For every species that makes up a land-cover class, the database contains the percent of the land-cover class ground area that is covered by the species and the foliar density of the species, D_i, which is the leaf biomass of the given species that is contained in each unit area of the land-cover class. D_i is defined as

$$D_i = \frac{A_i d_i}{A_{\text{total}}}, \tag{2}$$

where d_i is the leaf biomass of species i per unit area covered by species i, A_i the land-cover–class ground area covered by species i, and A_{total} the total ground area covered by the land-cover class. ($A_i\, A_{\text{total}}^{-1}$ is the percent of the area of the given land-cover class that is covered by species i.) The sum of the area fraction of all species in a land-cover class is the total percent vegetated area; the remaining percentage is assumed unvegetated. When linked to tables contained in GLOBEIS, the Wiedinmyer database also contains BVOC emission capacities (units: $\mu g\, C\, gdlm^{-1}\, h^{-1}$) for each of the contained 289 vegetation species.

2.2. Conversion of Wiedinmyer database to PFTs

We used the Wiedinmyer database to develop a data set that describes the Texas landscape in terms of CLM-compatible PFTs (Fig. 1). Every species contained in the Wiedinmyer database was assigned to one PFT. We assumed all PFTs in Texas are temperate (i.e., because the state is entirely located in the mid-latitudes, there are neither tropical PFTs nor boreal PFTs in Texas). A list of definitions of PFTs present in Texas can be found in the footnotes of Table 1.

Species in phylogenetic divisions Cycadophyta, Ginkgophyta, and Magnoliophyta were considered broadleaf; species in division Coniferophyta, needleleaf. To determine whether a species is evergreen or deciduous, we used the USDA Plants National Database (http://plants.usda.gov) as our primary source of information. Secondary sources included the Texas A&M Trees and Shrubs of Texas

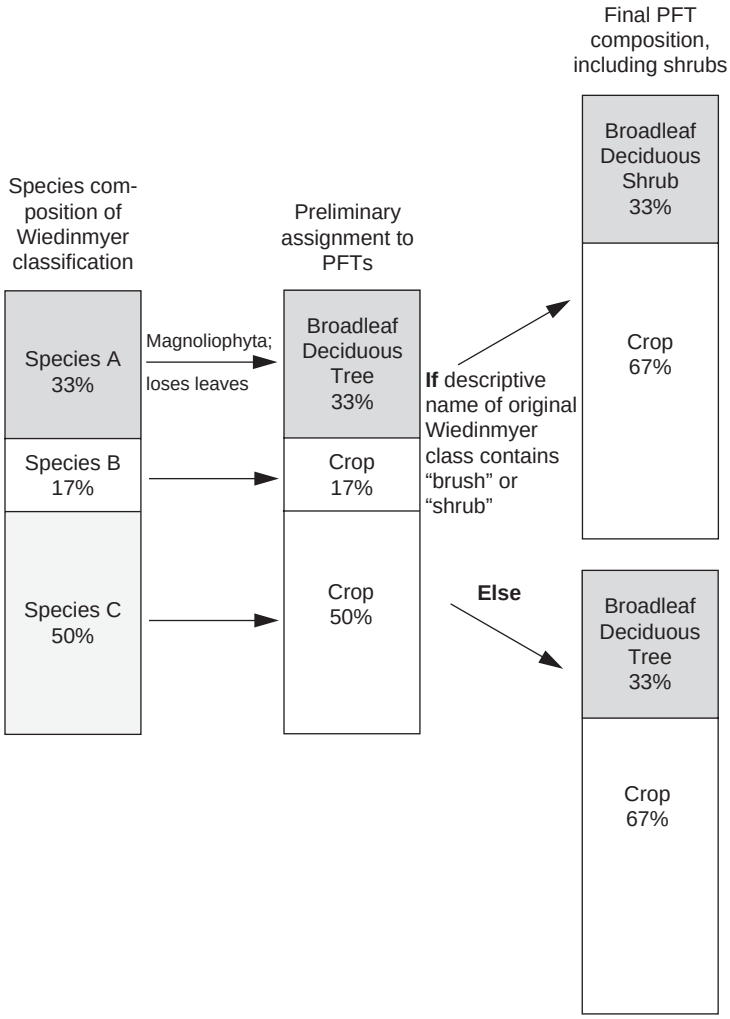

Fig. 1. Schematic diagram of the PFT conversion process. Percent area shown is percent of vegetated area. Schematic representation of the calculation of foliar density and total vegetated area is not included.

databases (http://aggie-horticulture.tamu.edu/ornamentals/natives/tamuhort.html) and the work of Stahl and McElvaney (2003). If information regarding the leaf life of a species was contradictory, priority was given to the information in the Plants National Database. If information was unavailable, the species was considered deciduous or evergreen based on the characteristics of plants sharing the same genus and based on local knowledge.

The Wiedinmyer database does not contain information that allows for objective description of species as trees or shrubs. In the initial conversion, all shrubs were considered trees. For example, *Atriplex canescens*, Four-Wing Saltbush, although morphologically a shrub, was considered a broadleaf deciduous tree (BDT) in the first analysis. After the initial conversion, all "trees" in Wiedinmyer land-cover classes whose descriptive names contained the words "Shrub", "Brush", or "Shrub and Brush" were reclassified as shrubs. (It is worthwhile to note that this method prevents the coexistence of trees and shrubs in a given $1 \times 1\text{-km}^2$ grid cell, which likely misrepresents reality in transitional regions such as the savannas of central Texas.) The standard initialization of the CLM does not contain a temperate needleleaf evergreen shrub (NES), but the prevalence of temperate evergreen coniferous shrub species (e.g., Alligator Juniper [*Juniperus deppeana*]) in some regions of western Texas justified the inclusion of NES as a component

Table 1
Comparison of BVOC emission capacities (ε_i, units: $\mu g\,C\,gdlm^{-1}\,h^{-1}$) for PFTs

Method	Plant functional type[a]									
	NET	NES[b]	NDT[b]	BET	BES	BDT	BDS	Crop	Grass (C_3, C_4)	Water[c]
Isoprene										
Levis et al.	2.0	2.0	0.0	24.0	24.0	24.0	24.0	0.0	0.0	0.0
CLM3, one region	0.1	0.1	0.2	44.6	12.6	43.1	3.8	0.0	0.0	2.5
CLM3, two regions										
West	0.1	0.1	0.0	44.8	13.5	26.2	4.1	0.0	0.0	0.0
East	0.1	0.1	0.2	44.6	0.8	45.5	2.2	0.0	0.0	2.5
Monoterpene										
Levis et al.	2.0	2.0	1.6	0.8	0.8	0.8	0.8	0.1	0.1	0.0
CLM3, one region	2.2	0.5	2.3	0.5	0.7	0.6	0.6	0.1	0.0	1.6
CLM3, two regions										
West	1.0	0.5	0.0	1.5	0.7	0.8	0.7	0.1	0.0	0.0
East	2.4	0.4	2.3	0.3	0.0	0.6	0.0	0.1	0.0	1.6
OVOC										
Levis et al.	1.0	1.0	1.0	1.0	1.0	1.0	1.0	1.0	1.0	0.0
CLM3, one region	1.9	1.3	1.3	2.0	0.7	2.1	1.1	0.0	0.0	1.8
CLM3, two regions										
West	2.1	1.3	0.0	2.0	0.7	2.8	1.3	0.0	0.0	0.0
East	1.9	1.1	1.3	2.0	0.1	2.0	0.1	0.1	0.0	1.8

Emission capacities shown are rounded to the nearest tenth, but non-rounded emission capacities were used when calculating statewide inherent emission rates.

[a]NET, needleleaf evergreen tree; NES, needleleaf evergreen shrub; NDT, needleleaf deciduous tree; BET, broadleaf evergreen tree; BES, broadleaf evergreen shrub; BDT, broadleaf deciduous tree; BDS, broadleaf deciduous shrub.

[b]For the calculations of statewide inherent fluxes using Levis et al.'s emission capacities, the NES emission capacity was assumed to have the same value as the Levis et al. emission capacity for NET. NDT (a temperate PFT) was assumed to have the same value as the Levis et al. emission capacity for boreal NDT.

[c]Water is not a PFT in CLM; however, in the Wiedinmyer database, water bodies can have BVOC-emitting capacity. Consequently, an emission capacity for water was calculated.

PFT. The standard initialization of CLM also does not contain a temperate needleleaf deciduous tree (NDT), but the presence of bald cypress (*Taxodium distichum*) in eastern Texas justified the addition of temperate NDT to the PFTs existing in Texas.

All crop species, regardless of photosynthetic pathway, were considered part of the same PFT (crop). Because the Wiedinmyer database does not provide species information for vegetation identified as "grass", we were unable to use the Wiedinmyer database to distinguish between C_3 and C_4 grasses. To define grass as C_3, C_4, or a C_3–C_4 mix, we followed the methods of Bonan et al. (2002). Grass populations in locations where the mean monthly temperature never reaches or exceeds 22 °C were defined as pure C_3. No location in Texas has meets the criteria to contain pure C_4 grass, which requires that mean monthly temperatures exceed 22 °C throughout the year. Remaining grasslands were considered to be 50% C_3 and 50% C_4. To approximate monthly mean temperature, we averaged PRISM 1971–2001 mean monthly maximum and minimum temperature data (see http://www.ocs.oregonstate.edu/prism). The native resolution of the PRISM grids was 4 km; we used nearest-neighborhood interpolation to obtain 1-km grids.

For each Wiedinmyer land-cover class, we calculated (1) the percent of ground area covered by every PFT and (2) the foliar density of each component PFT. The former was calculated by summing the area fraction (units: $m^2\,m^{-2}$) of all species in the class identified as a PFT. The later was defined as the sum of the foliar densities of all plant species contained within the land-cover class identified as a PFT. Fig. 1 shows a schematic diagram of the process, and Fig. 2 displays the resulting PFT distribution. Employing information contained within the Wiedinmyer database, we created gridded landunit-level maps of urban and water-covered areas in Texas.

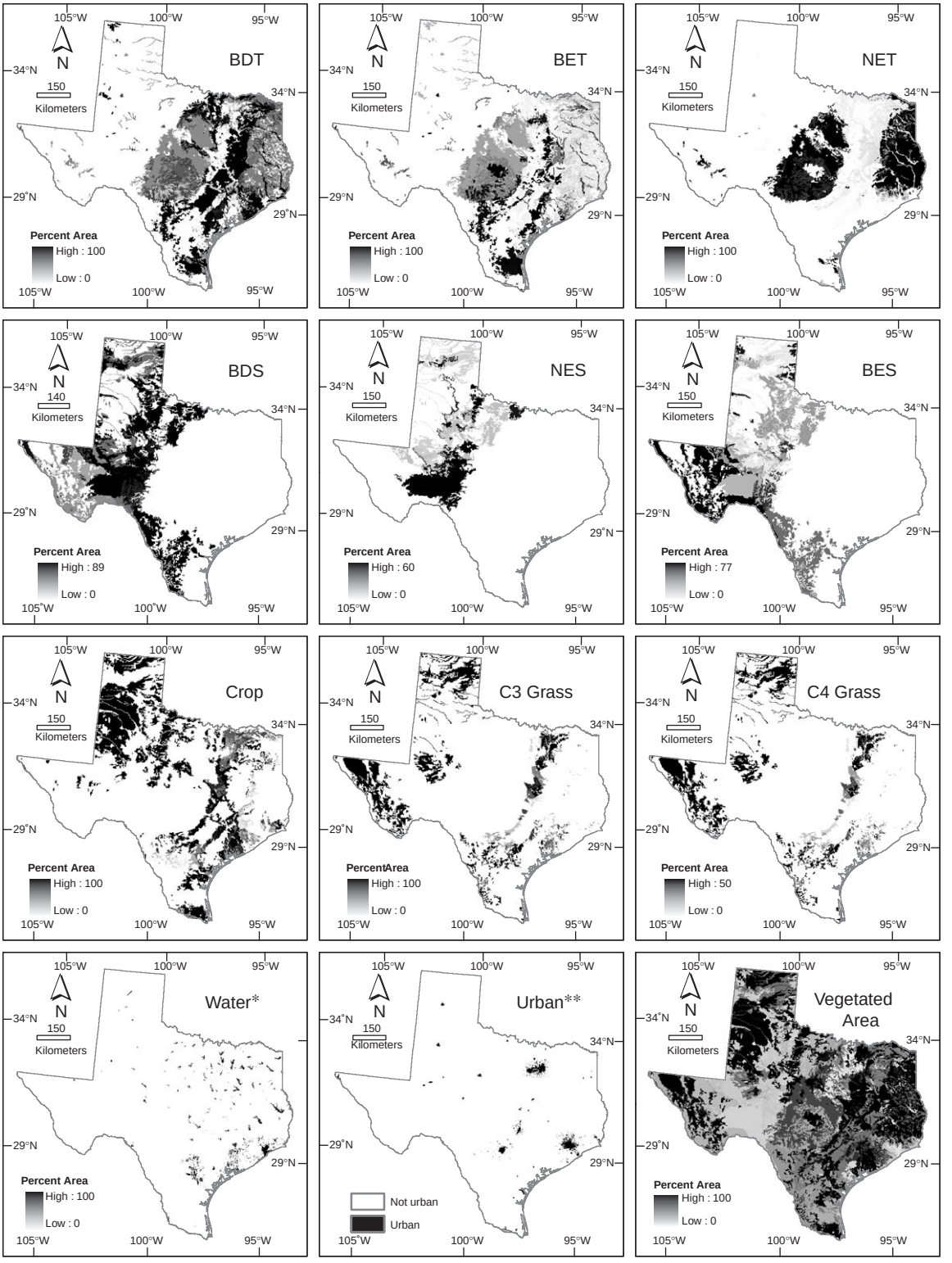

Fig. 2. Percent of vegetated area covered by different PFTs. The lower right-hand panel shows percent total vegetated area. NET, needleleaf evergreen tree; NES, needleleaf evergreen shrub; BET, broadleaf evergreen tree; BES, broadleaf evergreen shrub; BDT, broadleaf deciduous tree; BDS, broadleaf deciduous shrub. Because needleleaf deciduous trees are rare in Texas, their distribution is not shown. NES is not a PFT in the standard version of CLM3; see preceding section for discussion. *,** Water and Urban are landunit level land covers in CLM, not PFTs.

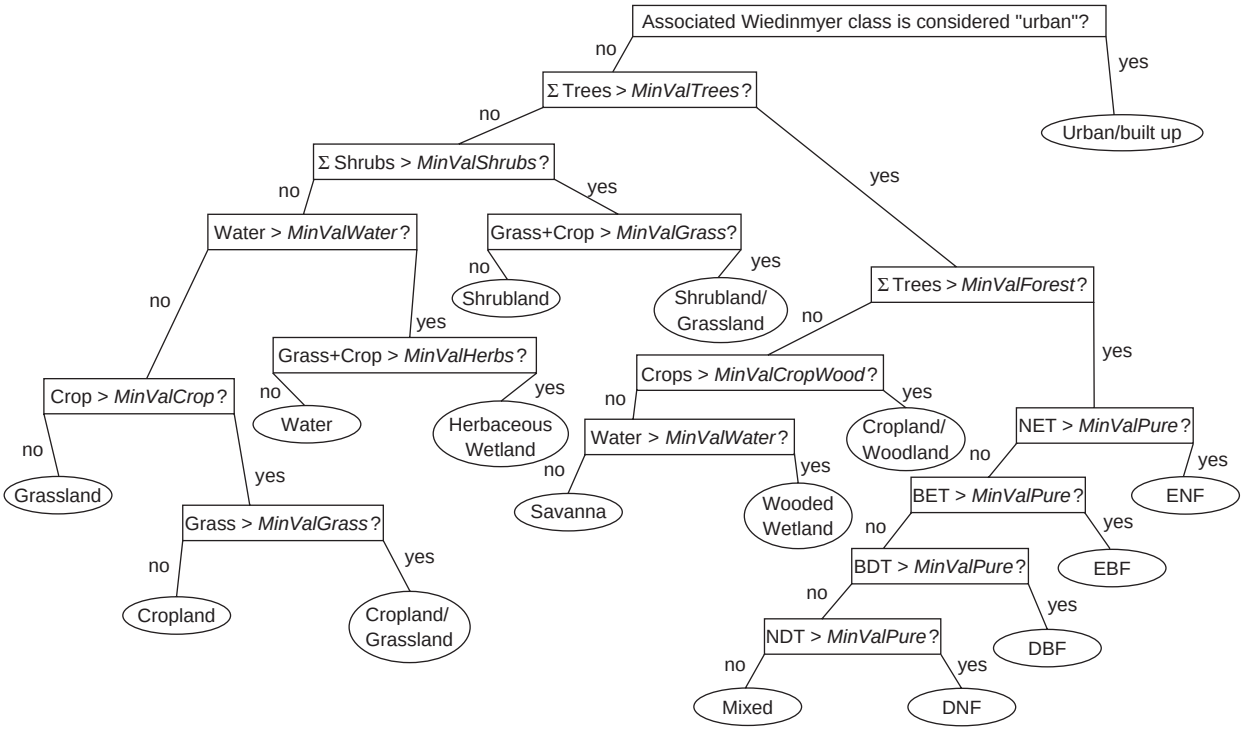

Fig. 3. Decision tree used to derive a Noah-compatible land-cover classification from the Wiedinmyer-based PFT database. In the diagram below, ENF, evergreen needleleaf forest; EBF, evergreen broadleaf forest; DBF, deciduous broadleaf forest; and DNF, deciduous needleleaf forest. "Mixed" is forest containing a mixture of trees in which no type (ENF, EBF, DNF, or DBF) exceeds the value chosen for "MinValPure". Breakpoint values are as follows: MinValTrees = 10; MinValForest = 50; MinValCropWood = 40; MinValShrubs = 10; MinValWater = 70; MinValCrop = 10; MinValGrass = 20; MinValHerbs = 10; MinValPure = 60.

2.3. Conversion of Wiedinmyer database to Noah-compatible land-cover types

Like many LSMs, Noah uses static land-cover types (e.g., "Mixed Forest", "Cropland/Grassland Mosaic") to represent surface vegetation. Because a Noah land-cover type can contain more than one type of plant (e.g., "Savanna" contains both grass and tree species), conversion from the species-based Wiedinmyer data set directly to Noah land-cover types could be accomplished only by using subjective methods. We chose instead to determine the distribution of Noah land-cover types in Texas by using the PFT percent composition information as input to a decision-tree algorithm (Fig. 3). The resulting database can be used as input to WRF–Noah version 2.1, the default version of which uses land-cover categories identical to those used in the USGS land-use/land-cover system (Anderson et al., 1976). Fig. 4 compares the Wiedinmyer-derived Noah land cover with the default USGS-based land cover.

Breakpoint values within the decision tree (e.g., "MinValTrees", the minimum percentage of tree cover required for a land-cover class to be considered a type of forest, savanna, wooded wetland, or a cropland–woodland mosaic; see legend of Fig. 3) were chosen so that the definitions of the land-cover classes were broadly consistent with the work of other researchers (e.g., Hansen et al., 2000) (Fig. 5).

2.4. Calculation of Texas-specific BVOC emission capacities

The CLM emissions module calculates BVOC fluxes for isoprene, monoterpene, and OVOCs, as well as for CO and ORVOCs. In the standard version of CLM3, emission capacities for CO and ORVOCs do not differ between PFTs. The GLOBEIS-linked Wiedinmyer database contains plant-species-specific emissions rates for only isoprene, monoterpene, and OVOCs. We calculated region-specific emission capacities for only these three

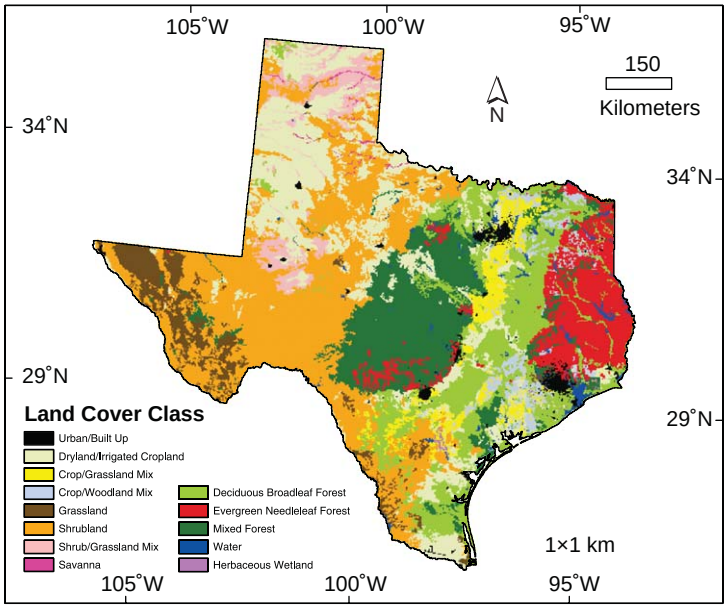

(A)

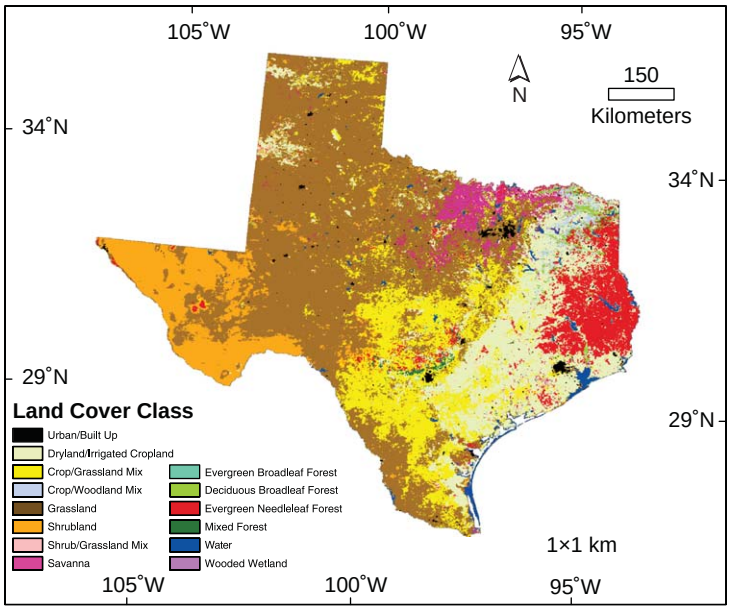

(B)

Fig. 4. Results of conversion of Wiedinmyer database to Noah land-cover (Panel A); default USGS-based Noah land-cover distribution (Panel B).

BVOC species. The emission capacity of PFT_x with respect to a single BVOC type, $\varepsilon_{\mathrm{PFT}x}$ (units: $\mu g\,C\,gdlm^{-1}\,h^{-1}$), was calculated as

$$\varepsilon_{\mathrm{PFT}_x} = \frac{F_{\mathrm{PFT}_x}}{W_{\mathrm{PFT}_x}}, \tag{3}$$

where F_{PFT_x} is the total BVOC emissions per hour emitted by PFT_x across Texas (units: $\mu g\,C\,h^{-1}$) and $W_{\mathrm{PFT}x}$ the total leaf biomass (gdlm) of PFT_i in Texas. We defined

$$F_{\mathrm{PFT}_x} = \sum_{j=1}^{n} A_j \left(\sum_{i=1}^{m_{\mathrm{PFT}_x}} \varepsilon_i D_i \right)_j, \tag{4}$$

where n is the number of land-cover classes in Texas, A_j the total area in Texas covered by

land-cover class j, m_{PFT_x} the number of species in land-cover class j identified as PFT_x, ε_i the emissions rate per unit biomass (units: $\mu g\,C\,gdlm^{-1}\,h^{-1}$) of the ith species identified as PFT_x in land-use code j, and D_i the foliar density (as defined in Eq. (2)) of the ith species in land-use code j. Fig. 5 shows the distribution of leaf biomass density, according to the Wiedinmyer database. We calculated

$$W_{\mathrm{PFT}x} = \sum_{j=1}^{n} A_j \left(\sum_{i=1}^{m_{\mathrm{PFT}_x}} D_i \right)_j, \quad (5)$$

where A_j, D_i, and m_{PFT_x} are as described above.

There exists significant variation in the emission capacity of the Texas-native plant species that compose each PFT. It is possible that plant-species' emission capacities vary regularly as a function of location within Texas. (For instance, species classified as BDT that are native to western Texas may have emission characteristics that differ significantly from those of species classified as BDT that are native to eastern Texas.) To explore this possibility, we derived two sets of region-specific PFT emission capacities for two sub-regions in Texas (eastern and western Texas). The 99th meridian formed the approximate boundary between the two sub-regions.

Table 1 compares the Levis et al. emission capacities with the region-specific emission capacities derived here. Following methods similar to those outlined above, we also derived region-specific emission capacities for use with the Noah land-cover database (Table 2).

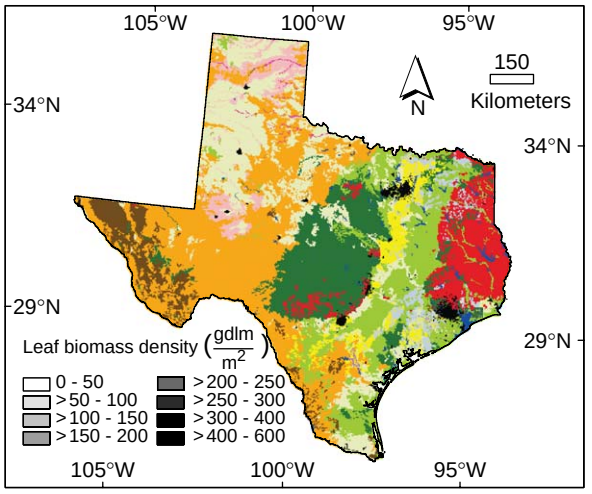

Fig. 5. Leaf biomass density ($gdlm\,m^{-2}$) according to the Wiedinmyer database.

2.5. Calculation of specific leaf area for use in Noah LSM and CLM model runs

The Levis et al. emissions module computes biogenic emissions as a function of leaf biomass density, but CLM tracks variations in vegetation biomass using leaf area index (units: $m^2\,leaf\,m^{-2}$-ground). Levis et al. assign each PFT a time-invariant specific leaf area (units: $m^2\,leaf\,gdlm^{-1}$), which allows for conversion between leaf area index and leaf biomass density (Foley et al., 1996; Levis et al., 2003). Using static leaf area index and leaf biomass density values provided in the Wiedinmyer database, we derived specific leaf area for each PFT and each Noah land-cover type using a biomass-weighted averaging method analogous to that used to derive region-specific BVOC emission capacities (Table 3).

Specific leaf area values are not necessary for evaluation of the region-specific emission capacities;

Table 2
BVOC emission capacities (ε_i, units: $\mu g\,C\,gdlm^{-1}\,h^{-1}$) for Noah land-cover types

Land cover[a]	Urban	Crop	Crop/Grass	Crop/Wood	Grass	Shrub	Shrub/Grass	Savanna	DBF	ENF	Mixed	Water	Herb. Wet.
Iso.[b]	30.1	0.1	0.0	12.1	0.0	8.0	0.1	0.0	36.7	12.2	15.0	2.2	1.4
Mono.[b]	0.8	0.1	0.1	0.3	0.0	0.9	0.2	0.0	0.5	2.6	0.6	1.4	0.9
OVOC[b]	1.7	0.1	0.0	0.7	0.0	1.4	1.3	0.0	1.8	1.8	1.8	1.6	1.1

[a]Urban, urban/built up; Crop, irrigated/dryland cropland; Crop/Grass, cropland/grassland mosaic; Crop/Wood, cropland/woodland mosaic; Shrub, shrubland; Shrub/Grass, shrubland/grassland mosaic; DBF, deciduous broadleaf forest; ENF, evergreen needleleaf forest; Mixed, mixed forest; Herb. Wet., herbaceous wetland. Deciduous needleleaf forest (DNF) and evergreen broadleaf forest (EBF) are not included in the above table because, in this analysis, nowhere in Texas is identified as EBF or DNF. "Mixed" is mixed forest, which is any mixture of DBF, EBF, ENF, and/or DNF, in which no tree type covers a percentage of the vegetated area that exceeds MinValPure (see Fig. 3).

[b]Emission capacities shown are rounded to the nearest tenth, but raw values for emission capacities were used to calculate statewide inherent emission rates.

Table 3
Specific leaf area (SLA) (m^2 leaf $gdlm^{-1}$) for CLM plant functional types and Noah LSM land-cover types

	CLM plant functional type[a]								
	NET	NES[b]	NDT[b]	BET	BES	BDT	BDS	Crop	Grass (C_3,C_4)
Levis et al.	0.0125	0.0125	0.0125	0.0250	0.0250	0.0250	0.0250	0.0200	0.0200
CLM3, one region	0.0139	0.0141	0.0243	0.0317	0.0185	0.0295	0.0157	0.0308	0.0200[c]
CLM3, two regions									
East	0.0130	0.0121	0.0243	0.0292	0.0009	0.0277	0.0013	0.0293	0.0200[c]
West	0.0223	0.0142	n/a	0.0483	0.0198	0.0422	0.0180	0.0314	0.0200[c]

Noah LSM land-cover type[a]

Urban	Crop	Crop/Grass	Crop/Wood	Grass[d]	Shrub	Shrub/Grass	Savanna	DBF	ENF	Mixed	Herb. Wet.
0.0228	0.0295	0.0223	0.0277	0.0056	0.0227	0.0188	0.0236	0.0258	0.0090	0.0223	0.0390

[a]See first footnote of Table 1 for full names corresponding to the PFT acronyms; see first footnote of Table 2 for full names corresponding to land-cover type abbreviated names.

[b]Temperate NDT and NES do not exist in the standard version of CLM3; specific leaf areas for NDT and NES are assumed to be equal to the Levis et al. specific leaf area for NET.

[c]The specific leaf area calculated for grass species using the data provided in the Wiedinmyer database (SLA ≈ 0.00001) was unreasonably small; consequently, we recommend the use of the standard-CLM specific leaf area for grass.

[d]Because the specific leaf area calculated for grass is unreasonably small (see previous footnote), the specific leaf area calculated for grasslands (which contain a large percentage of grass species) may also be a significant underestimate.

however, we present them here because they are necessary components of model simulations that use the Texas-specific emission capacities derived in this study. It should be noted that the Noah LSM uses greenness fraction, not leaf area index, to track variations in biomass. The specific leaf area values for each Noah land-cover code shown in Table 3 must, therefore, be used in conjunction with a mechanism to convert greenness fraction to leaf area index.

2.6. Calculation of inherent BVOC flux

We used inherent BVOC flux as a measure by which to evaluate the accuracy of the emission capacities derived here. Inherent flux, F, for each type of BVOC was defined as

$$F = \sum_{i=1}^{n} \varepsilon_i D_i, \tag{6}$$

where n is the number of species or land-cover types covering the grid cell, ε_i the emission capacity of species, land-cover type, or PFT i, and D_i the foliar density of i (as defined in Eq. (2)). In all cases, we used the foliar density information provided in the Wiedinmyer database to compute inherent BVOC flux. For computations using PFTs, we considered D_i to be the sum of the foliar densities of all species in a grid cell identified as PFT i. Because Noah land-cover classes are a static composition of plant types ($n = 1$ in Eq. (6)), the inherent flux for a given 1×1-km^2 grid cell is $F = \varepsilon D$, where ε is the emission capacity for the land-cover class and D the grid-cell–mean foliar density (as defined in Eq. (2)). Evaluation of results using inherent BVOC flux calculated using a standard leaf biomass density map allowed us to focus entirely on variation in BVOC emission resulting from differences in emission capacities, neglecting differences resulting from environmental variation.

3. Results and discussion

We defined the total inherent BVOC flux as the sum of the inherent fluxes for isoprene, monoterpene, and OVOCs. Fig. 6 shows the statewide total inherent BVOC fluxes calculated using the Levis et al. emission capacities and the Wiedinmyer-derived CLM-compatible land-cover data set (“Levis”); calculated using the one-region, Texas-specific PFT emission capacities and the CLM-compatible data set (“One-region”); calculated using the two-region, Texas-specific PFT emission capacities and the CLM-compatible data set (“Two-region”); and calculated using the Texas-specific

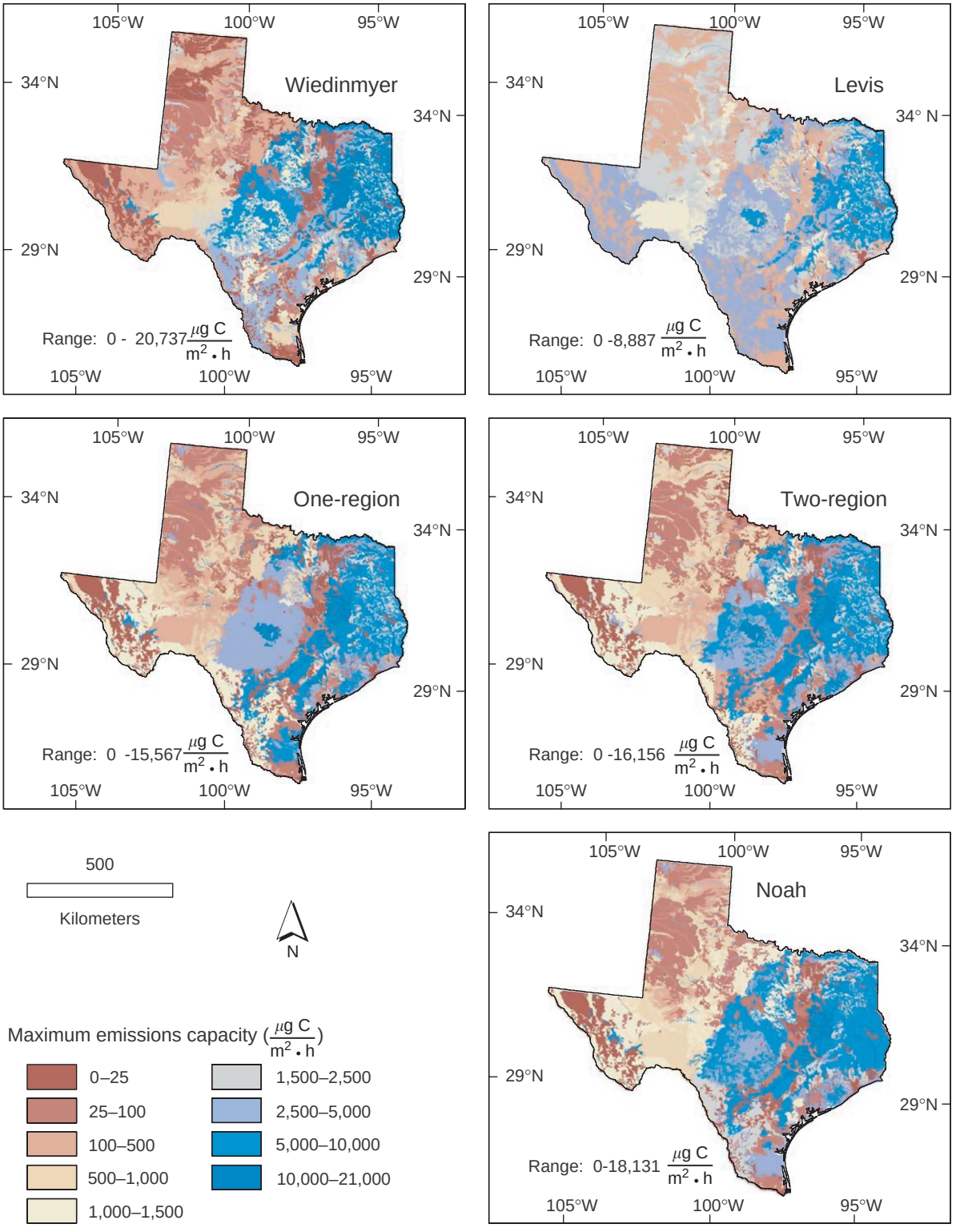

Fig. 6. Total inherent BVOC emission capacity (sum of the inherent emission capacity for isoprene, monoterpene, and OVOC). The panel labels (e.g., ''Levis'') describe the method used to calculate the total inherent BVOC emission capacity.

Table 4
Univariate statistics for inherent BVOC[a] fluxes in Texas

Method used to calculate inherent fluxes	Range of inherent BVOC fluxes ($\mu g\,C\,m^{-2}\,h^{-1}$)	Mean inherent flux ($\mu g\,C\,m^{-2}\,h^{-1}$)	SD	Skewness	Kurtosis
Wiedinmyer database (''observations'') calculated directly from species	0–20737	2689	3973	1.8005	2.7289
CLM: Levis et al. emission capacities (globally constant)	0–8887	2285	1928	0.8920	0.3370
CLM: Texas-specific emission capacities (one region)	0–15567	2689	3453	1.4303	1.3434
CLM: Texas-specific emission capacities (two regions)	0–16156	2689	3531	1.5253	1.6656
Noah: Texas-specific emission capacities	0–18,131	2689	3360	0.0165	−0.7756

[a]Inherent BVOC fluxes are the sum of the inherent fluxes of isoprene, monoterpene, and OVOC.

Table 5
Correlation and error of calculated inherent BVOC fluxes

Method used to calculate BVOC emissions	Pearson's product-moment correlation coefficient (r)	Mean absolute error[a]	Root mean square error[a]
Calculated directly from species-specific emission capacities.	1.0000	0	0
CLM: Levis et al. emission capacities (globally constant)	0.8502	1668	2577
CLM: TX-specific emission capacities (one region)	0.8875	1111	1832
CLM: TX-specific emission capacities (two regions)	0.8899	1085	1813
Noah: TX-specific emission capacities	0.8893	945	1629

[a]As defined in Willmott (1982).

Noah land-cover emission capacities and the Noah-compatible land-cover data set (''Noah''). When evaluating the ability of the region-specific emission capacities to represent BVOC emissions in Texas, we considered the inherent BVOC flux derived directly from the species-specific emission capacities and the species-based land-cover map to be the ''observed'' data (''Wiedinmyer'' in Fig. 6). Although the spatial distribution of the ''Levis'' inherent fluxes is qualitatively similar to that of the observed data, the inherent fluxes calculated with region-specific emission capacities greatly improve the LSMs' ability to simulate BVOC emissions.

Table 4 shows univariate statistics for the results shown in Fig. 6; Table 5 displays the correlation coefficient, the mean absolute error (MAE), and the root mean square error for the results shown in Fig. 6. The inherent BVOC fluxes calculated using the region-specific emission capacities are better correlated with the observed fluxes than the inherent fluxes derived using Levis et al. emission capacities. A comparison of the MAE values for the inherent flux data sets shows that regional emission capacities greatly improve the ability of LSMs to simulate inherent BVOC fluxes, and consequently, BVOC emissions.

All MAE values for the region-specific inherent fluxes are 41% or less of the mean inherent flux, and all are an order of magnitude lower than the range of values in the observed data sets. This compares quite favorably to the MAE of the ''Levis'' inherent emission rates, which is 73% of the data set's mean value and 19% of the range. When the Texas-specific emission capacities derived in this study are used in climate and weather simulations, the spatial distribution of BVOC emissions will better reflect observed emissions, which will consequently improve the spatial accuracy of the modeled climate and weather processes that depend on biogenic emissions (e.g., secondary organic aerosol formation and tropospheric ozone production).

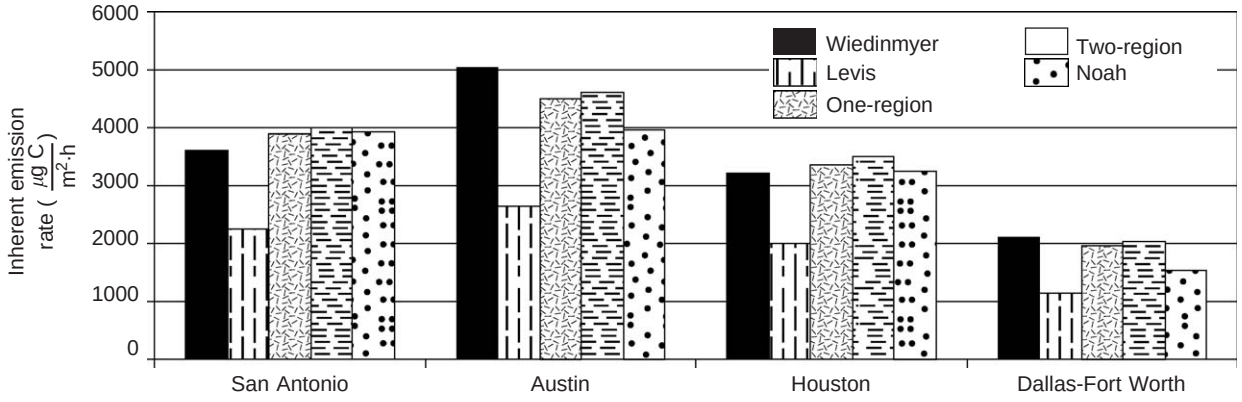

Fig. 7. Comparison of the average inherent BVOC flux in four Texas cities calculated using the "observed" species data ("Wiedinmyer"), the globally constant PFT-specific emission capacities used by Levis et al. ("Levis"), the Wiedinmyer-derived land-cover-type emission capacities for use in the Noah LSM ("Noah"), and the Wiedinmyer-derived PFT-specific emission capacities calculated using statewide plant-species data ("One-region") and species data from east and west Texas ("Two-region").

Use of the globally constant emission capacities from Levis et al. substantially underestimates the total BVOC emissions in Texas: the cumulative statewide inherent BVOC flux calculated using the Levis et al. emission capacities was only 85% of the observed (Wiedinmyer) cumulative statewide inherent flux. Because the method presented here preserves the total mass of BVOCs emitted from the landscape under normalized temperature and PAR conditions, each of the three Wiedinmyer-derived inherent flux distributions has cumulative statewide inherent BVOC fluxes that are identical to that computed using the original Wiedinmyer data set (Table 4). However, the different spatial distribution of inherent fluxes obtained using the Wiedinmyer-derived emission capacities results in different average BVOC fluxes at regional scales. Fig. 7 shows the average inherent BVOC flux for four major metropolitan areas in Texas. In each of the four urban areas, use of any of the three Wiedinmyer-derived emission capacities ("One-region", "Two-region", and "Noah" in Fig. 7) substantially improves upon the average inherent flux calculated using Levis et al.'s values ("Levis" in Fig. 7).

Use of emission capacities derived from two sub-regions improves the spatial distribution of inherent emission capacities, especially in central Texas; however, the improvement in accuracy is not as great as one might expect. The lower foliar density of the west-Texas landscape (Fig. 4) likely accounts for a greater portion of the difference in the inherent fluxes than do the slight variations in the regional emission capacities between the species native to east and west Texas (Table 1). Different choice of sub-regions (e.g., north and south Texas) might also provide a greater increase in accuracy.

Further improvement of BVOC-emission simulation could likely be gleaned by the addition of "high-emitting" land-cover types to CLM and Noah. For example, a BDT that shares all physical parameters except its isoprene emission capacity with the CLM-standard BDT would represent BDT species with anomalously high-isoprene emission capacities (e.g., oak species). Emission capacities calculated for the "high-isoprene" BDT and the standard BDT would consequently be more representative of the emission capacities of their constituent species. Similar high-emitting PFTs for plant species with anomalous monoterpene or OVOC emission capacities would improve model simulation results in regions where such species are prevalent. Future work will include the addition of such land-cover types to both CLM and Noah.

The analysis presented here focuses on the relative improvement gained by using region-specific, species-based emission capacities. Evaluation of the absolute improvement in accuracy gained by using the ecologically based emission capacities is challenging because of a dearth of large-scale, high-resolution empirical data. However, the ecologically based, "bottom-up" method presented here is presumably more plausible than the "top-down" assignation of emission capacities to land-cover types used in similar modeling studies (e.g., Levis et al.; Naik et al., 2004). Means for evaluation of the

absolute accuracy of the magnitude and spatial distribution of BVOC emissions and the weather and climatic processes that depend upon them is an area of ongoing research.

Application of this method to other regions may be hindered by the lack of availability of detailed, species-based land-cover databases such as the Wiedinmyer et al. database. Less-detailed species-based vegetation data sets, such as the 1-km Biogenic Emissions Landcover Database (Kinnee et al., 1997), can be used in similar bottom-up fashion to derive region-specific emission capacities for LSMs. In the US, myriad less extensive vegetation species databases sponsored by state and federal agencies (e.g., the Calflora vegetation species database [http://www.calflora.org/]) augment the species-distribution data available to researchers.

The BVOC emission capacities derived for Texas may be representative of those in humid-to-arid transition zones and may thus be transferable to regions with similar climate. Sen et al. (2001) used observational data from five sites, each representative of a different biome, to calibrate the vegetation parameters for a general circulation model; their model simulations using the field-calibrated vegetation data showed more skill than did those using standard parameters. A similar approach using BVOC emission capacities derived from representative regions might improve modeled BVOC emissions in continental- and global-scale simulations without requiring detailed, species-based vegetation maps for all regions. However, because BVOC emissions vary at the species level, extensive further study is necessary to determine whether such generalization is defensible.

As a derivative product, this study inherits all uncertainty associated with the input Wiedinmyer land-cover data set. As Wiedinmyer et al. (2000, 2001b) point out, the uncertainty associated with the original data set is difficult to quantify. The extensive field surveys undertaken by Wiedinmyer and colleagues and the field-surveys underpinning the 10 land-cover data sets that formed the basis for the Wiedinmyer data set serve to lessen the associated uncertainty; however, field-survey verification of the Wiedinmyer data set was limited to central and eastern Texas, where BVOC emissions rates are high. Although ground surveys for the data sets underpinning the Wiedinmyer data set were generally not as localized, the uncertainty of the Wiedinmyer data set increases from east to west (Wiedinmyer et al., 2001b).

The accuracy of the inherent BVOC fluxes calculated here depends on the accuracy of the emissions data contained within GLOBEIS. Intraspecies variation in BVOC emissions and the dependence of emissions on environmental variables lessens the transferability of site-specific, BVOC-emissions measurements to regional modeling applications. Intraspecies variation is likely considerable: e.g., Funk et al. (2005) found that under normal climate conditions, isoprene emissions from different red oak trees within a single stand differed by a factor of two. Interspecies variation also introduces uncertainty. The number of vegetation species in Texas is considerably greater than the 289 species contained within the Wiedinmyer database; for most species in Texas, observed BVOC emission capacities do not exist. New field and laboratory data (e.g., Geron et al., 2001) combined with methods for assigning BVOC emission capacities to species for which no measurements exist (e.g., Karlik et al., 2002) will lessen but not eliminate this uncertainty.

Another source of uncertainty inherent to the method presented here results from the use of a time-varying property (leaf biomass density) to derive a time-invariant property (PFT-specific emission capacity). The emission capacities for use with the Noah-compatible database also depend on the selection of the breakpoint values in the decision-tree algorithm used to derive the Noah-compatible database from the PFT database. Detailed factorial analysis could help determine the most accurate breakpoint values (e.g., Henderson-Sellers, 1993).

4. Summary and conclusions

The CLM-compatible and Noah-compatible data sets developed for this study can be used for a wide variety of regional weather and climate simulations. They are the first high-resolution, ground-referenced vegetation data sets for Texas for use in LSMs.

Use of the PFT emission capacities that are standard in CLM3 likely underestimates the cumulative BVOC emissions from vegetation in Texas and fails to capture the range of inherent BVOC fluxes. Region-specific emission capacities, calculated using either one region or two smaller subregions, improve the ability of LSMs to simulate the inherent BVOC flux. The correlation between the observed inherent fluxes and the inherent fluxes calculated using region-specific emission capacities ($r = 0.89$) is better than that between observations

and the fluxes calculated using the CLM standard emission capacities ($r = 0.85$). Use of region-specific emission capacities lessens the MAE of the calculated inherent flux. (MAE is $1668\,\mu g\,C\,m^{-2}\,h^{-1}$ when using standard CLM emission capacities; 1111 and $1085\,\mu g\,C\,m^{-2}\,h^{-1}$ when using region-specific CLM emission capacities derived from one and two regions, respectively; and $945\,\mu g\,C\,m^{-2}\,h^{-1}$ when using region-specific Noah emission capacities.) Sub-division of Texas into two smaller sub-regions improved the accuracy of the spatial distribution of inherent emission capacities. However, for regions the size of Texas, a single set of regional PFT BVOC emission capacities may be used without a large compromise in the overall accuracy of the spatial distribution of emissions.

Region-specific, species-derived BVOC emission capacities, when used in conjunction with detailed land-cover data sets, allow for reasonably accurate simulation of BVOC emissions on a regional scale. Climate and weather models that employ region-specific BVOC emission capacities will be better equipped to study the impact of biogenic emissions on atmospheric processes and the influence of atmospheric variation on biogenic emissions.

Acknowledgements

The Environmental Protection Agency provided funding for this research (Grant No. RD83145201). We thank Christine Wiedinmyer, Victoria Junquera, and William Vizuete for providing us with the original data set and for their insight and assistance over the course of the research. We would also like to thank Robert Dickinson for valuable comments regarding methods for improving simulation of BVOC emissions in LSMs. This manuscript was substantially improved by the insightful comments of two anonymous reviewers and of Lauren Greene.

References

Abbot, D.S., et al., 2003. Seasonal and interannual variability of North American isoprene emissions as determined by formaldehyde column measurements from space. Geophysical Research Letters 30 (17), 1886.

Anderson, J.R., et al., 1976. A land use and land cover classification system for use with remote sensor data: US Geological Survey Professional Paper 964, 28 p.

Andreaevc, M.O., Crutzen, P.J., 1997. Atmospheric aerosols: biogeochemical sources and role in atmospheric chemistry. Science 276, 1052–1058.

Bonan, G.B., et al., 2002. Landscapes as patches of plant functional types: an integrating concept for climate and ecosystem models. Global Biogeochemical Cycles 16.

Chen, F., Dudhia, J., 2001. Coupling an advanced land surface-hydrology model with the Penn State-NCAR MM5 modeling system. Part I: model implementation and sensitivity. Monthly Weather Review 129, 569–585.

Claeys, M., et al., 2004. Formation of secondary organic aerosols through photooxidation of isoprene. Science 303, 1173–1176.

Foley, J.A., et al., 1996. An integrated biosphere model of land surface processes, terrestrial carbon balance, and vegetation dynamics. Global Biogeochemical Cycles 10 (4), 603–628, doi:10.1029/96GB02692.

Funk, J.L., et al., 2005. Variation in isoprene emission from *Quercus rubra*: sources, causes, and consequences for estimating fluxes. Journal of Geophysical Research—Atmospheres 110, D04301.

Geron, C., et al., 2001. Isoprene emission capacity for US tree species. Atmospheric Environment 35, 3341–3352.

Grell, G.A., Dudhia, J., Stauffer, D.R., 1995. A description of the fifth-generation Penn State/NCAR mesoscale model. NCAR Technical Note, NCAR-TN 398 + STR. Accessed 19 October 2005 at: 〈http://www.mmm.ucar.edu/mm5/documents/mm5-desc-pdf/cover.pdf〉.

Guenther, A., 2002. The contribution of reactive carbon emissions from vegetation to the carbon balance of terrestrial ecosystems. Chemosphere 49, 837–844.

Guenther, A.B., Monson, R.K., Fall, R., 1991. Isoprene and monoterpene emission rate variability: observations with eucalyptus and emission rate algorithm development. Journal of Geophysical Research—Atmospheres 96 (D6), 10799–10808.

Guenther, A., et al., 1995. A global-model of natural volatile organic-compound emissions. Journal of Geophysical Research—Atmospheres 100, 8873–8892.

Hakola, H., et al., 2003. Seasonal variation of VOC concentrations above a boreal coniferous forest. Atmospheric Environment 37, 1623–1634.

Hansen, M.C., et al., 2000. Global land cover classification at 1 km spatial resolution using a classification tree approach. International Journal of Remote Sensing 21, 1331–1364.

Henderson-Sellers, A., 1993. A factorial assessment of the sensitivity of the BATS land-surface parameterization scheme. Journal of Climate 6, 227–247.

Karlik, J.F., et al., 2002. A survey of California plant species with a portable VOC analyzer for biogenic emission inventory development. Atmospheric Environment 36, 5221–5233.

Kavouras, I.G., Mihalopoulos, N., Stephanou, E.G., 1998. Formation of atmospheric particles from organic acids produced by forests. Nature 395, 683–686.

Kinnee, E., Geron, C., Pierce, T., 1997. United States land use inventory for estimating biogenic ozone precursor emissions. Ecological Applications 7 (1), 46–58.

Levis, S., et al., 2003. Simulating biogenic volatile organic compound emissions in the community climate system model. Journal of Geophysical Research—Atmospheres 108 (D21), 4659.

Naik, V., et al., 2004. Sensitivity of global biogenic isoprenoid emissions to climate variability and atmospheric CO_2. Journal of Geophysical Research—Atmospheres, doi:10.1029/2003JD004236.

Oleson, K.W., et al., 2004. Technical Description of the Community Land Model. National Center for Atmospheric

Research, Boulder, CO (174pp). Accessed 16 May 2004 at: ⟨http://www.cgd.ucar.edu/tss/clm/distribution/clm3.0/TechNote/CLM_Tech_Note.pdf⟩.

Plaza, J., et al., 2005. Field monoterpene emission of Mediterranean oak (*Quercus ilex*) in the central Iberian Peninsula measured by enclosure and micrometeorological techniques: observation of drought stress effect. Journal of Geophysical Research—Atmospheres 110, D03303.

Sen, O.L., et al., 2001. Impact of field-calibrated vegetation parameters on GCM climate simulations. Quarterly Journal of the Royal Meteorological Society 127, 1199–1223.

Skamarock, W.C., et al., 2005. A Description of the Advanced Research WRF, version 2. Accessed 19 October 2005 at: ⟨http://www.wrf-model.org/wrfadmin/docs/arw_v2.pdf⟩.

Stahl, C., McElvaney, R., 2003. The Trees of Texas: an Easy Guide to Leaf Identification. Texas A&M University Press, College Station, TX (288pp, pp. 1–288).

Wiedinmyer, C., et al., 2000. Biogenic hydrocarbon emission estimates for North Central Texas. Atmospheric Environment 34, 3419–3435.

Wiedinmyer, C., et al., 2001a. Measurement and analysis of atmospheric concentrations of isoprene and its reaction products in central Texas. Atmospheric Environment 35, 1001–1013.

Wiedinmyer, C., et al., 2001b. A land use database and examples of biogenic isoprene emission estimates for the state of Texas, USA. Atmospheric Environment 35, 6465–6477.

Willmott, C.J., 1982. Some comments on the evaluation of model performance. Bulletin of the American Meteorological Society 63, 1309–1313.

Yarwood, G., Wilson, G., Emery, C., Guenther, A., 1999. Development of GloBEIS—a state of the science biogenic emissions modeling system. Final Report, Prepared for Texas Natural Resource Conservation Commission, Provided by the author.